AIAA 2002-1573

A MULTIFUNCTIONAL INTERFACE METHOD FOR COUPLING FINITE ELEMENT AND FINITE DIFFERENCE METHODS: TWO-DIMENSIONAL SCALAR-FIELD PROBLEMS

Jonathan B. Ransom*
NASA Langley Research Center
Hampton, VA 23681-2199, U.S.A.

Abstract

A multifunctional interface method with capabilities for variable-fidelity modeling and multiple method analysis is presented. The methodology provides an effective capability by which domains with diverse idealizations can be modeled independently to exploit the advantages of one approach over another. The multifunctional method is used to couple independently discretized subdomains, and it is used to couple the finite element and the finite difference methods. The method is based on a weighted residual variational method and is presented for two-dimensional scalar-field problems. A verification test problem and a benchmark application are presented, and the computational implications are discussed.

Introduction

Accurate response characterization is needed early in the design and analysis cycle to investigate rapidly novel and revolutionary aerospace and ground vehicle design concepts. Mathematical modeling approximations are considered that range from simple handbook equations, empirically derived relations, spreadsheets, and design charts to complex continuous and discrete simulation models. Integrated computational methods with multiple capabilities and with diverse engineering applications provide the enabling technologies to assimilate variable-fidelity, multi-disciplinary data rapidly at an early stage in the design. These methods allow rapid design trade-offs between cost and performance. Based on the insight provided by these simulations, design uncertainties and risk assessment may be evaluated. Moreover, methodology that allows different mathematical modeling approximations of the physical phenomena and among multiple engineering disciplines can be very advantageous.

One class of methods for obtaining the desired modeling flexibility in the analysis of complex systems that has received recent attention is generally called interface methods. These methods, through the subdivision of a single domain into multiple subdomains, are used to couple independently discretized models or to couple different mathematical modeling methods or approximations, and exploit the advantages of one approach over another. Examples of methods that couple different independently discretized models include global/local approaches[1-4] and finite element coupling methods[5-10]. Examples of methods that couple different modeling methods include finite element and boundary element methods[11-14], finite element and Rayleigh-Ritz approximations[15], finite element and finite difference methods[16,17], finite element and analytical solutions[18], and finite element and equivalent plate solutions[19]. These interface methods facilitate the discretization of geometry by providing a capability to model independently the regions of interest, increasing the discretization fidelity or enhancing the mathematical approximation only in desired domains. A major feature of the methods is the accurate mapping of field quantities across the respective interface, whether the interface is one among diverse mathematical approximations or among diverse disciplines. Many of the interface methods are specific to a single spatial modeling approach (*i.e.*, finite element method) or discipline, which limits their applicability to a wide range of applications in engineering science.

This paper presents a multifunctional interface method with capabilities for variable-fidelity modeling and multiple method analysis. An interface method referred to in the literature as interface technology[9,10] was developed for coupling independently discretized finite element models and is well suited for extensions

* Aerospace Engineer, Analytical and Computational Methods Branch, Member AIAA

to multiple method and multidisciplinary analysis. Therefore, the interface technology is the concept upon which the multifunctional capability presented in this work is built. The basic concept of the interface technology was discussed by Housner and Aminpour [9] and subsequently, developed, implemented and validated by Aminpour et al.[10], and Ransom et al. [20]. The method has been shown to be computationally efficient while preserving solution accuracy, however, its demonstration has been limited to solid mechanics problems.

The purpose of this paper is to investigate multifunctional interface methods, as described herein that address the engineering design and analysis needs of multidisciplinary problems in engineering science. Fundamental relationships will be discussed among underlying engineering science and mechanics principles, computational methods, variable-fidelity models, and multiple methods using basic two-dimensional scalar-field problems from continuum mechanics. A multifunctional approach for scalar-field problems is developed, described, and demonstrated on problems in engineering science. A multifunctional formulation is presented along with a discussion of the spatial modeling and the computational implications. The multifunctional method is used to couple independently discretized subdomains and to couple the finite element and the finite difference methods. Numerical results for a verification test case and a representative scalar-field problem are presented.

Overview of the Multifunctional Approach for Scalar-field Problems

Methods of approximation such as Ritz, Galerkin, and other weighted residual methods are based on weak statements of the differential equations governing the system response. The scalar-field problem is a basic form of the governing differential equations; and thus, it lends itself to forming the mathematical foundation for the general methodology developed herein. Representative examples of scalar-field differential equations in two dimensions are considered, and the mathematical statement of the multifunctional approach is formulated.

The general form of the differential equation describing a scalar-field problem for domain Ω (see Figure 1(a)) is given by the Poisson equation, which is of the form

$$-\nabla\cdot\left(k\nabla u\right)=Q \quad \text{in } \Omega \tag{1}$$

subject to the natural boundary condition, $k\frac{\mathrm{d}u}{\mathrm{d}n}+h\left(u-u_\infty\right)=q$ on Γ^s, and essential boundary condition, $u=\bar{u}$ on Γ^p. The normal derivative, $\frac{\mathrm{d}u}{\mathrm{d}n}=\frac{\partial u}{\partial x}\mathbf{n}_x+\frac{\partial u}{\partial y}\mathbf{n}_y$, and $\mathbf{n}_x$ and $\mathbf{n}_y$ are the components of the outward normal vector, **n**, to the bounding surface, Γ, of domain, Ω. In Eq. (1), the variables k and Q are known coefficients, and the primary variable or dependent variable is u, which is a function of the independent variables, x and y. In the natural boundary condition, the variables, h and u_∞, are the convection coefficient, and the far-field value of the primary variable, respectively. The terms, q, $k\frac{\partial u}{\partial x}$, and $k\frac{\partial u}{\partial y}$ are the secondary variables that may be described on a portion of the boundary, Γ^s. The primary variable, u, is specified on the boundary, Γ^p, and its prescription to the boundary value, $\bar{u}$, constitutes the essential boundary condition. The complete boundary is defined as $\Gamma=\Gamma^p+\Gamma^s$.

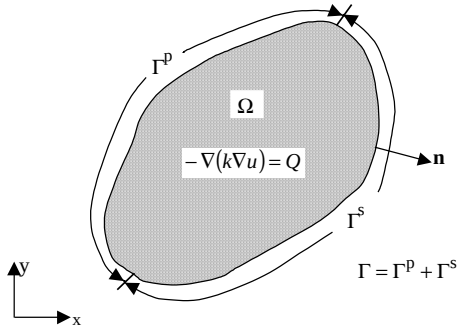

(a) Geometric representation

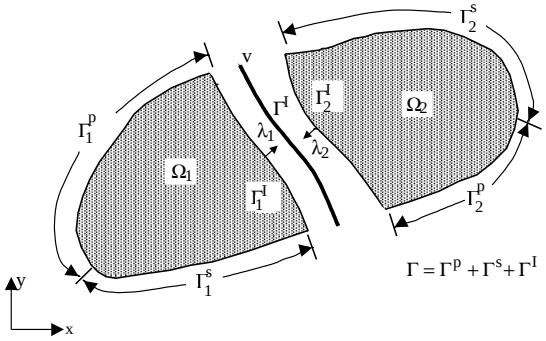

(b) Boundary Definitions for subdomains

Figure 1. Geometric Representation and Boundary Definitions of Two-Dimensional Domain.

Equations of the type of Eq. (1) arise in many fields of engineering science such as elasticity, heat

transfer, fluid mechanics, and electrostatics. Reddy[21] has tabulated several examples of engineering fields in which the analytical description of the physical process is described by Eq. (1). In this paper, the Poisson equation is applied to selected problems in the solid mechanics.

Multifunctional Formulation

The method of weighted residuals is used extensively in fluid mechanics; and thus, the potential problem is formulated from this perspective. The general weighted residual formulation for a single domain is presented in reference 22. The multifunctional formulation provides a capability to subdivide a domain into multiple, independently idealized subdomains, which allows the use of independently generated models, multiple levels of spatial discretization, and different mathematical approximations among the subdomains. These attributes facilitate the use of higher localized fidelity for increased solution accuracy and the ability to capitalize on the advantages of one mathematical approximation compared to another. The method is quite similar to the subdomain collocation approach in which a domain is divided into subdomains, and the residual is made orthogonal to a weight function and set to zero in an integral sense over each subdomain. Here, methodology is presented formulating the general method of weighted residuals for multiple domains by considering the Poisson equation, Eq. (1) for a two-dimensional domain for the field variable, *u*.

For simplicity, the multiple-domain formulation is presented for two subdomains, Ω_1 and Ω_2 (see Figure 1(b)). Independent approximations and weight functions are assumed in each of the subdomains and continuity conditions are used to provide for a continuous solution across the subdomain interfaces. Thus, Eq. (1) is satisfied in each subdomain, independently, *i.e.*,

$$-\nabla\cdot\left(k_i\nabla u_i\right)=Q_i \quad \text{in } \Omega_i$$

or for uniform constant, *k*, in each subdomain

$$-k_i\nabla^2 u_i = Q_i \quad \text{in } \Omega_i$$

subject to the boundary conditions on the subdomain boundaries, Γ_i.

As a result of the subdomain modeling, the solution of the problem involves an interior surface interface boundary, Γ_i^{I}, and the information transfer across the boundary. Hence, the boundary surface for the i^{th} subdomain is given by $\Gamma_i=\Gamma_i^p+\Gamma_i^s+\Gamma_i^{\mathrm{I}}$. The boundary conditions for the i^{th} subdomain may be written as

$$u_i-\overline{u}_i=0 \quad \text{on } \Gamma_i^p \quad \text{and} \quad k_i\frac{\mathrm{d}u_i}{\mathrm{d}n}-\overline{q}_i=0 \quad \text{on } \Gamma_i^s .$$

The residual, $R_i=-k_i\nabla^2 u_i-Q_i$, for each domain is orthogonalized by a set of weight functions, Φ_i which yields

$$\int_{\Omega_i}\left(-k_i\nabla^2 u_i-Q_i\right)\Phi_i\,\mathrm{d}\Omega_i=0$$

where the approximate solution, $\tilde{u}_i$, is sought. Using the general form outlined in reference 22 for the single-domain formulation and considering an approximate solution, $\tilde{u}_i$, that automatically satisfies the essential boundary conditions, we may write the general integral form of the differential equation governing the potential flow for subdomain *i* as

$$\begin{aligned}&\int_{\Omega_i}\Phi_i\left[-k_i\left(\frac{\partial^2\tilde{u}_i}{\partial x^2}+\frac{\partial^2\tilde{u}_i}{\partial y^2}\right)-Q_i\right]\mathrm{d}\Omega_i+\\&\int_{\Gamma_i^s}\overline{\Phi}_i\left(k_i\frac{\mathrm{d}\tilde{u}_i}{\mathrm{d}n}-\overline{q}_i\right)\mathrm{d}\Gamma_i^s=0\end{aligned} \tag{2}$$

where $\dfrac{\mathrm{d}\tilde{u}_i}{\mathrm{d}n}=\dfrac{\partial\tilde{u}_i}{\partial x}\mathbf{n}_{x_i}+\dfrac{\partial\tilde{u}_i}{\partial y}\mathbf{n}_{y_i}$ and the residual in the satisfaction of the natural boundary conditions is orthogonalized by a secondary set of weight functions $\overline{\Phi}_i$.

The order of differentiation on the primary variable in the integral equations, Eq. (2), is reduced to obtain the weak formulation. In addition, for simplicity in the subsequent development, the tilde, (˜), denoting the approximated values of the primary variables, u_1 and u_2, will be omitted. Utilizing the divergence theorem, Eq. (2) can be rewritten, for subdomain *i*, yielding

$$\begin{aligned}&\int_{\Omega_i}k_i\left(\frac{\partial u_i}{\partial x}\frac{\partial\Phi_i}{\partial x}+\frac{\partial u_i}{\partial y}\frac{\partial\Phi_i}{\partial y}\right)\mathrm{d}\Omega_i-\\&\oint_{\Gamma_i}k_i\left(\frac{\partial u_i}{\partial x}\mathbf{n}_{x_i}+\frac{\partial u_i}{\partial y}\mathbf{n}_{y_i}\right)\Phi_i\mathrm{d}\Gamma_i-\\&\int_{\Omega_i}Q_i\Phi_i\mathrm{d}\Omega_i+\int_{\Gamma_i^s}\left(k_i\frac{\mathrm{d}u_i}{\mathrm{d}n}-\overline{q}_i\right)\overline{\Phi}_i\mathrm{d}\Gamma_i^s=0 \quad .\end{aligned} \tag{3}$$

Recall that the boundary integral on Γ_i, may be expressed as the sum of boundary integrals associated

with the specified primary variable, Γ_i^p, specified secondary variable, Γ_i^s, and the interior surface interface boundary, Γ^{I}, with $\boldsymbol{\Phi}_i = \mathbf{0}$ on Γ_i^p. Moreover, since $\boldsymbol{\Phi}_i$ and $\overline{\boldsymbol{\Phi}}_i$, are arbitrary, they may be chosen, such that, $\boldsymbol{\Phi}_i = \overline{\boldsymbol{\Phi}}_i$. Thus, Eq. (3) can be rewritten, for subdomain *i*, as

$$\int_{\Omega_i} k_i \left(\frac{\partial u_i}{\partial x}\frac{\partial \boldsymbol{\Phi}_i}{\partial x} + \frac{\partial u_i}{\partial y}\frac{\partial \boldsymbol{\Phi}_i}{\partial y} \right) \mathrm{d}\Omega_i - \int_{\Gamma^{\mathrm{I}}} k_i \frac{\mathrm{d}u_i}{\mathrm{d}n} \boldsymbol{\Phi}_i \mathrm{d}\Gamma^{\mathrm{I}} - \int_{\Gamma_i^s} \overline{q}_i \boldsymbol{\Phi}_i \mathrm{d}\Gamma_i^s - \int_{\Omega_i} Q_i \boldsymbol{\Phi}_i \mathrm{d}\Omega_i = 0 \quad . \quad (4)$$

To enforce interdomain continuity on the primary variable, a boundary condition on the boundary, Γ^{I}, is used by introducing a third approximation field in terms of an additional primary variable, *v*, (see Figure 1(b)) which gives rise to the continuity requirement

$$v - u_1 = 0 \quad \text{on} \quad \Gamma^{\mathrm{I}} \quad \text{and} \quad v - u_2 = 0 \quad \text{on} \quad \Gamma^{\mathrm{I}}.$$

These constraints can be satisfied in the integral sense as

$$\int_{\Gamma^{\mathrm{I}}} \lambda_1 (v - u_1) \mathrm{d}\Gamma^{\mathrm{I}} = 0 \quad \text{on} \quad \Gamma^{\mathrm{I}}$$

and

$$\int_{\Gamma^{\mathrm{I}}} \lambda_2 (v - u_2) \mathrm{d}\Gamma^{\mathrm{I}} = 0 \quad \text{on} \quad \Gamma^{\mathrm{I}} \quad (5)$$

where λ_1 and λ_2 are Lagrange multipliers or weight functions related to the secondary variable along the interface. To enforce reciprocity of the secondary variable (*i.e.*, fluxes or tractions) along the common subdomain boundary, an additional continuity requirement is specified. These secondary variables, $\hat{q}_1$ and $\hat{q}_2$, are assumed to be independent of each other. These independent approximations give rise to continuity requirements along the interface

$$\hat{q}_1 + \hat{q}_2 = 0 \quad \text{on} \quad \Gamma^{\mathrm{I}}.$$

These constraints can be satisfied in the integral sense as

$$\int_{\Gamma^{\mathrm{I}}} \hat{\lambda} (\hat{q}_1 + \hat{q}_2) \mathrm{d}\Gamma^{\mathrm{I}} = 0 \quad \text{on} \quad \Gamma^{\mathrm{I}} \quad (6)$$

where $\hat{\lambda}$ is a Lagrange multiplier or weight function related to the primary variable along the interface. The integral form of Eqs. (4), (5), and (6) provides the basis for the subsequent spatial modeling approximations. The multifunctional approach developed provides a mechanism for coupling subdomains that have been discretized with diverse spatial modeling approaches. Of the many spatial modeling approaches, this paper will focus on the finite element and the finite difference methods and their associated coupling using the multifunctional approach developed.

Eqs. (4), (5), and (6) are used to provide the mathematical basis for the development. In previous work by Aminpour et al.[10], a similar formulation based on the principle of minimum potential energy is developed and subsequently implemented in the form of an element[20]. In that work as is the case in this study, the interdomain interface boundary is discretized with a mesh of evenly-spaced pseudo-nodes (open circles in Figure 2) that need not be coincident with any of the interface nodes (filled circles in the figure) of any of the subdomains. In this paper, the methodology has been extended further to encompass diverse types of spatial modeling methods as is indicated conceptually in Figure 2.

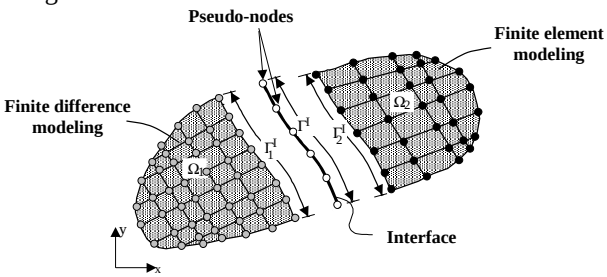

Figure 2. Interface Definition.

The generalized element equations may be obtained by introducing the continuity requirements into the weighted residual statement. Eqs. (4), (5), and (6) can be rewritten over an element domain as

$$\int_{\Omega_i^e} k_i \left(\frac{\partial u_i}{\partial x}\frac{\partial \boldsymbol{\Phi}_i}{\partial x} + \frac{\partial u_i}{\partial y}\frac{\partial \boldsymbol{\Phi}_i}{\partial y} \right) \mathrm{d}\Omega_i^e - \int_{\Gamma^{\mathrm{I}^e}} \hat{q}_i \boldsymbol{\Phi}_i \, \mathrm{d}\Gamma^{\mathrm{I}^e} - \int_{\Gamma_i^{s^e}} \overline{q}_i \boldsymbol{\Phi}_i \, \mathrm{d}\Gamma_i^{s^e} - \int_{\Omega_i^e} Q_i \boldsymbol{\Phi}_i \mathrm{d}\Omega_i^e = 0$$

and

$$\int_{\Gamma^{\mathrm{I}^e}} \lambda_1 (v - u_1) \mathrm{d}\Gamma^{\mathrm{I}^e} = 0, \quad \int_{\Gamma^{\mathrm{I}^e}} \lambda_2 (v - u_2) \mathrm{d}\Gamma^{\mathrm{I}^e} = 0, \quad \int_{\Gamma^{\mathrm{I}^e}} \hat{\lambda} (\hat{q}_1 + \hat{q}_2) \mathrm{d}\Gamma^{\mathrm{I}^e} = 0. \quad (7)$$

Note that in the potential energy formulation[10], the continuity of the secondary variables is satisfied

through the subsidiary conditions obtained through the minimization of the potential energy. In this weighted residual formulation, the continuity of the secondary variables is satisfied in a weighted residual sense and the Lagrange multipliers, λ_i and $\hat{\lambda}$, are represented by weight functions related to the secondary and primary variables, respectively.

The form of the equations for finite element and finite difference field approximations differs by the form of the element shape functions and the approximation selected for the weight functions, Φ. For the generalized element expansion of subdomain *i*, the independent approximations for the element primary variables, (*i.e.*, displacements or velocities), interface secondary variables (*i.e.*, tractions or fluxes), the weight functions associated with the primary and secondary variables, and the interface variables are, respectively

$$\mathbf{u}_i = \mathbf{N}_i \mathbf{u}_{e_i} \quad ; \quad \hat{\mathbf{q}}_i = \mathbf{R}_i \boldsymbol{\alpha}_i \quad ; \quad \lambda_i = \mathbf{R}_i \; ; \; \hat{\lambda} = \mathbf{T}$$
$$\text{and} \quad \mathbf{v} = \mathbf{T}\mathbf{u}_\mathrm{I}$$

where $\boldsymbol{\alpha}_i$ is a vector of unknown coefficients associated with the secondary variables, $\hat{\mathbf{q}}_i$, and $\mathbf{N}_i$, $\mathbf{R}_i$, and $\mathbf{T}$ are matrices of interpolation functions for the element primary and secondary variables, and the primary variables along the interface, respectively. The interpolation functions in the matrices $\mathbf{R}_i$ are assumed to be constants for linear elements and linear functions for quadratic elements. The interpolation functions in the matrix $\mathbf{T}$ are cubic spline functions. Substituting these approximations into Eqs. (7) yields integral equations in terms of the weight function, Φ, which are given by

$$\left[\int_{\Omega_i^e} k_i \left(\frac{\partial \mathbf{N}_i^\mathrm{T}}{\partial x}\frac{\partial \boldsymbol{\Phi}_i}{\partial x} + \frac{\partial \mathbf{N}_i^\mathrm{T}}{\partial y}\frac{\partial \boldsymbol{\Phi}_i}{\partial y} \right) \mathrm{d}\Omega_i^e \right] \mathbf{u}_{e_i} -$$
$$\left[\int_{\Gamma^{\mathrm{I}^e}} \boldsymbol{\Phi}_i^\mathrm{T} \mathbf{R}_i \, \mathrm{d}\Gamma^{\mathrm{I}^e}\right] \boldsymbol{\alpha}_i = \int_{\Omega_i^e} \boldsymbol{\Phi}_i^\mathrm{T} Q_i \mathrm{d}\Omega_i^e + \int_{\Gamma_i^{s^e}} \boldsymbol{\Phi}_i^\mathrm{T} \overline{q}_i \, \mathrm{d}\Gamma_i^{s^e}$$

and

$$-\left[\int_{\Gamma^{\mathrm{I}^e}} \mathbf{R}_1{}^\mathrm{T} \mathbf{N}_1 \, \mathrm{d}\Gamma^{\mathrm{I}^e}\right] \mathbf{u}_{e_1} + \left[\int_{\Gamma^{\mathrm{I}^e}} \mathbf{R}_1{}^\mathrm{T} \mathbf{T} \, \mathrm{d}\Gamma^{\mathrm{I}^e}\right] \mathbf{u}_\mathrm{I} = 0$$
$$-\left[\int_{\Gamma^{\mathrm{I}^e}} \mathbf{R}_2{}^\mathrm{T} \mathbf{N}_2 \, \mathrm{d}\Gamma^{\mathrm{I}^e}\right] \mathbf{u}_{e_2} + \left[\int_{\Gamma^{\mathrm{I}^e}} \mathbf{R}_2{}^\mathrm{T} \mathbf{T} \, \mathrm{d}\Gamma^{\mathrm{I}^e}\right] \mathbf{u}_\mathrm{I} = 0$$
$$\left[\int_{\Gamma^{\mathrm{I}^e}} \mathbf{T}^\mathrm{T} \mathbf{R}_1 \, \mathrm{d}\Gamma^{\mathrm{I}^e}\right] \boldsymbol{\alpha}_1 + \left[\int_{\Gamma^{\mathrm{I}^e}} \mathbf{T}^\mathrm{T} \mathbf{R}_2 \, \mathrm{d}\Gamma^{\mathrm{I}^e}\right] \boldsymbol{\alpha}_2 = 0$$

or symbolically,

$$\mathbf{k}_{e_i} \mathbf{u}_{e_i} + \mathbf{k}_{s_i} \boldsymbol{\alpha}_i = \mathbf{f}_{e_i}$$
$$\mathbf{k}_{p_i} \mathbf{u}_{e_i} + \mathbf{k}_{\mathrm{I}_i}^\mathrm{T} \mathbf{u}_\mathrm{I} = 0$$

and

$$\sum_{i=1}^{2} \left(\mathbf{k}_{\mathrm{I}_i} \boldsymbol{\alpha}_i \right) = 0$$

where, for i=1,2,

$$\mathbf{k}_{\mathbf{e}_i} = \int_{\Omega_i^e} k_i \left(\frac{\partial \mathbf{N}_i^\mathrm{T}}{\partial x}\frac{\partial \boldsymbol{\Phi}_i}{\partial x} + \frac{\partial \mathbf{N}_i^\mathrm{T}}{\partial y}\frac{\partial \boldsymbol{\Phi}_i}{\partial y} \right) \mathrm{d}\Omega_i^e \; ,$$

$$\mathbf{k}_{\mathbf{p}_i} = -\int_{\Gamma^{\mathrm{I}^e}} \mathbf{R}_i^\mathrm{T} \mathbf{N}_i \mathrm{d}\Gamma^{\mathrm{I}^e} \quad ,$$

$$\mathbf{k}_{\mathbf{s}_i} = -\int_{\Gamma^{\mathrm{I}^e}} \boldsymbol{\Phi}_i^\mathrm{T} \mathbf{R}_i \, \mathrm{d}\Gamma^{\mathrm{I}^e} \; , \quad \mathbf{k}_{\mathrm{I}_i} = \int_{\Gamma^{\mathrm{I}^e}} \mathbf{T}^\mathrm{T} \mathbf{R}_i \mathrm{d}\Gamma^{\mathrm{I}^e} \quad ,$$

and

$$\mathbf{f}_{\mathbf{e}i} = \int_{\Omega_i^e} \Phi_i^\mathrm{T} Q_i \mathrm{d}\Omega_i^e + \int_{\Gamma_i^{s^e}} \boldsymbol{\Phi}_i^\mathrm{T} \overline{q}_i \, \mathrm{d}\Gamma_i^{s^e}$$

Moreover, integration over the common subdomain boundary, Γ^I, is considered only for element edges along that boundary.

Assembling the element equations over the entire domain, enforcing continuity of the primary and secondary variables only within each subdomain and assembling the contributions along the element edges on the common subdomain boundary, and noting that $\mathbf{u}_{\mathbf{e}_1}$ and $\mathbf{u}_{\mathbf{e}_2}$, and $\mathbf{f}_{\mathbf{e}_1}$ and $\mathbf{f}_{\mathbf{e}_2}$, and $\boldsymbol{\alpha}_1$ and $\boldsymbol{\alpha}_2$ are completely uncoupled, yields the system of equations given by

$$\begin{bmatrix} \mathbf{K}_1 & \mathbf{0} & \mathbf{0} & \mathbf{K}_{s_1} & \mathbf{0} \\ \mathbf{0} & \mathbf{K}_2 & \mathbf{0} & \mathbf{0} & \mathbf{K}_{s_2} \\ \mathbf{0} & \mathbf{0} & \mathbf{0} & \mathbf{K}_{\mathrm{I}_1} & \mathbf{K}_{\mathrm{I}_2} \\ \mathbf{K}_{p_1} & \mathbf{0} & \mathbf{K}_{\mathrm{I}_1}^\mathrm{T} & \mathbf{0} & \mathbf{0} \\ \mathbf{0} & \mathbf{K}_{p_2} & \mathbf{K}_{\mathrm{I}_2}^\mathrm{T} & \mathbf{0} & \mathbf{0} \end{bmatrix} \begin{Bmatrix} \mathbf{u}_1 \\ \mathbf{u}_2 \\ \mathbf{u}_\mathrm{I} \\ \boldsymbol{\alpha}_1 \\ \boldsymbol{\alpha}_2 \end{Bmatrix} = \begin{Bmatrix} \mathbf{f}_1 \\ \mathbf{f}_2 \\ \mathbf{0} \\ \mathbf{0} \\ \mathbf{0} \end{Bmatrix}$$

or symbolically $\begin{bmatrix} \mathbf{K} & \mathbf{0} & \mathbf{K}_\mathrm{s} \\ \mathbf{0} & \mathbf{0} & \mathbf{K}_\mathrm{I} \\ \mathbf{K}_\mathrm{p} & \mathbf{K}_\mathrm{I}^\mathrm{T} & \mathbf{0} \end{bmatrix} \begin{Bmatrix} \mathbf{u} \\ \mathbf{u}_\mathrm{I} \\ \boldsymbol{\alpha} \end{Bmatrix} = \begin{Bmatrix} \mathbf{f} \\ \mathbf{0} \\ \mathbf{0} \end{Bmatrix}$ (8)

where $\mathbf{K}$, $\mathbf{u}$, and $\mathbf{f}$ are the assembled stiffness matrix, vector of primary variables and force vector for the entire structure, and $\mathbf{K}_\mathrm{p}$, $\mathbf{K}_\mathrm{s}$, $\mathbf{K}_\mathrm{I}$, $\mathbf{u}_\mathrm{I}$, and $\boldsymbol{\alpha}$ are the assembled $\mathbf{K}_{p_i}$, $\mathbf{K}_{s_i}$, $\mathbf{K}_{\mathrm{I}_i}$, $\mathbf{u}_\mathrm{I}$, and $\boldsymbol{\alpha}_i$ for all interfaces. Eq. (8) is obtained from the individual weighted residual expressions over each of the subdomains and the constraint integrals.

Multiple-Domain Modeling - Homogeneous Discretization

In the context of this work, homogeneous discretization approaches make use of a single discretization method among all subdomains in which the domain is subdivided. For the finite element development, the weight functions are taken to be the finite element shape functions (*i.e.*, $\mathbf{\Phi}_i = \mathbf{N}_i$). For the finite difference development, the weight functions are taken to be the Dirac delta function (*i.e.*, $\mathbf{\Phi}_i = \delta_i(x - x_i, y - y_i)$). Thus, stiffness matrices, $\mathbf{k}_{\mathbf{e}_i}$ and $\mathbf{k}_{\mathbf{s}_i}$, and force vector, $\mathbf{f}_{\mathbf{e}_i}$, are given in terms of the weight functions. The form of the coupling element matrices, $\mathbf{k}_{\mathbf{p}_i}$ and $\mathbf{k}_{\mathrm{I}_i}$, that are not in terms of the weight functions are independent of the method of discretization. That is,

$$\mathbf{k}_{\mathbf{p}_i} = -\int_{\Gamma^{\mathrm{I}^e}} \mathbf{R}_i^{\mathrm{T}} \mathbf{N}_i \, \mathrm{d}\Gamma^{\mathrm{I}^e} \quad \text{and} \quad \mathbf{k}_{\mathrm{I}_i} = \int_{\Gamma^{\mathrm{I}^e}} \mathbf{T}^{\mathrm{T}} \mathbf{R}_i \, \mathrm{d}\Gamma^{\mathrm{I}^e}$$

are of the same form for the finite element and finite difference discretizations. However, since the element shape functions, $\mathbf{N}_i$, differ for the two methods, the interface matrices, $\mathbf{k}_{\mathbf{p}_i}$, in general, are not identical. Moreover, in the finite element development, at the element level $\mathbf{k}_{\mathrm{s}_i} = \mathbf{k}_{\mathrm{p}_i}^{\mathrm{T}}$, and at the global system level $\mathbf{K}_{\mathrm{s}_i} = \mathbf{K}_{\mathrm{p}_i}^{\mathrm{T}}$. By contrast, in the finite difference development, at the element level $\mathbf{k}_{\mathrm{s}_i} \neq \mathbf{k}_{\mathrm{p}_i}^{\mathrm{T}}$, and at the global system level $\mathbf{K}_{\mathrm{s}_i} \neq \mathbf{K}_{\mathrm{p}_i}^{\mathrm{T}}$. Hence, for the finite difference method, the global system level matrices are not symmetric. The multifunctional derivation is general as it allows for the coupling of the primary variables to an independent approximation. This attribute is particularly important in the heterogeneous discretization approach described in the next section.

Multiple-Domain Modeling - Heterogeneous Discretization

Heterogeneous discretization approaches make use of different discretization methods for at least two of the subdomains in which the domain is subdivided. There are many combinations of spatial modeling approaches; however, this work focuses on the coupling of the finite element and finite difference methods. The multifunctional weighted residual formulation of Eq. (8) is used. Considering two domains, shown in Figure 1(b), subdomain 1 is assumed to be discretized using the finite element method, and subdomain 2 is assumed to be discretized using the finite difference method. The set of element matrices becomes a hybrid of the matrices from the finite element method and the finite difference method, and

$$\mathbf{k}_{\mathbf{e}_1} = \int_{\Omega_1^e} k_1 \left(\frac{\partial \mathbf{N}_1^{\mathrm{T}}}{\partial x} \frac{\partial \mathbf{N}_1}{\partial x} + \frac{\partial \mathbf{N}_1^{\mathrm{T}}}{\partial y} \frac{\partial \mathbf{N}_1}{\partial y} \right) \mathrm{d}\Omega_1^e$$

and

$$\mathbf{k}_{\mathbf{e}_2} = k_2 \left(\left. \frac{\partial^2 \mathbf{N}_2^{\mathrm{T}}}{\partial x^2} \right|_{\substack{x=x_i \\ y=y_i}} + \left. \frac{\partial^2 \mathbf{N}_2^{\mathrm{T}}}{\partial y^2} \right|_{\substack{x=x_i \\ y=y_i}} \right),$$

$$\mathbf{k}_{\mathbf{s}_1} = -\int_{\Gamma^{\mathrm{I}^e}} \mathbf{N}_1^{\mathrm{T}} \mathbf{R}_1 \, \mathrm{d}\Gamma^{\mathrm{I}^e} \quad \text{and} \quad \mathbf{k}_{\mathbf{s}_2} = -\mathbf{R}_2(x_i, y_i) \,, \quad (9)$$

$$\mathbf{f}_{\mathbf{e}1} = \int_{\Omega_1^e} \mathbf{N}_1^{\mathrm{T}} Q_1 \mathrm{d}\Omega_1^e + \int_{\Gamma_1^{s^e}} \mathbf{N}_1^{\mathrm{T}} \overline{q}_1 \mathrm{d}\Gamma_1^{s^e}$$

and

$$\mathbf{f}_{\mathbf{e}2} = Q_2(x_i, y_i) + \overline{q}_2(x_i, y_i),$$

and for the two domains, i=1,2,

$$\mathbf{k}_{\mathbf{p}_i} = -\int_{\Gamma^{\mathrm{I}^e}} \mathbf{R}_i^{\mathrm{T}} \mathbf{N}_i \mathrm{d}\Gamma^{\mathrm{I}^e} \quad \text{and} \quad \mathbf{k}_{\mathrm{I}_i} = \int_{\Gamma^{\mathrm{I}^e}} \mathbf{T}^{\mathrm{T}} \mathbf{R}_i \, \mathrm{d}\Gamma^{\mathrm{I}^e} \,.$$

The multifunctional modeling approach has been generalized such that it is applicable to both homogeneous and heterogeneous discretization approaches.

Computational Implications

Computational implications are discussed for the generalized system of equations, Eqs. (8). Implications specific to a discretization approach are highlighted, where appropriate. The assembled stiffness matrix **K** is a block diagonal matrix containing the stiffness matrices $\mathbf{K}_i$ of each of the subdomains along its block diagonal. The interface "stiffness" matrix thus contains coupling terms that augment the stiffness matrices of the subdomains along the interface. Due to the use of Lagrange multipliers in the constraint conditions, the systems are neither banded nor positive definite. Therefore, standard Cholesky solvers can not be used, unless pivoting is performed to obtain the solution. In addition, due to the generalization for the finite difference approximations, the system of equations is not necessarily symmetric due to different off-diagonal submatrices, $\mathbf{K}_{\mathrm{p}}$ and $\mathbf{K}_{\mathrm{s}}$. The system unknowns in Eq. (8) consist of both primary and secondary variables given by the potential function, *u*, and the secondary variable coefficients, $\boldsymbol{\alpha}$, respectively. Generally, the terms in the coupling matrices, $\mathbf{K}_{\mathrm{s}_i}$, are of the magnitude of the length of the interdomain boundary, which results in a marked difference in the magnitude of the off-diagonal terms of the system matrix compared to its diagonal terms. This characteristic produces an ill-conditioned matrix whose solution can cause numerical difficulties for some general-purpose

solvers. Hence, the coupling matrix should be scaled such that its terms are of the same magnitude as the subdomain stiffness. The upper diagonal submatrix blocks contain uncoupled subdomain stiffness matrices. The symmetry of the subdomain matrix is determined by the choice of the weight function, Φ. For the finite element discretization, the subdomain matrices are symmetric. However, due to the elimination of fictitious nodes for the imposition of boundary conditions and loads in the finite difference discretization, the subdomain stiffness matrices, $\mathbf{K}_i$, generally are not symmetric, but they are positive definite and sparse. The coupling is accomplished through the introduction of the terms in the matrices, $\mathbf{K}_{p_i}$, $\mathbf{K}_{s_i}$, and $\mathbf{K}_I$. The number of additional degrees of freedom associated with the interface is generally small in comparison with the total number of degrees of freedom in the subdomains. Thus, modeling flexibility is provided at a relatively small computational expense that may be reduced additionally as the efficiency of new solution algorithms for the system of equations in Eqs. (8) is increased.

Numerical Results

The multifunctional methodology for the two-dimensional scalar-field problem is demonstrated on a verification patch test case and a benchmark problem (*i.e.*, a torsion problem). The applications are described, and the associated results and salient features are discussed. Finite difference and finite element solutions for single- and multiple-domain configurations are presented to provide benchmark solutions for the multifunctional approach using homogeneous and heterogeneous spatial discretizations. The finite element models use four-node Lagrange isoparametric finite elements, and the finite difference models use a five-point template to approximate the governing differential equation. A general-purpose finite element code, COMET/AR[23], is used to generate the finite element stiffness matrices. The mathematical computing program MATLAB® is used to generate the finite difference matrices and the interface coupling matrices and to solve the resulting system of equations.

Patch Test Problems

The fundamental concept of the patch test for the scalar-field problem herein is to subject a domain to boundary conditions that engender a linear or quadratic primary variable field and a constant or linear secondary variable field throughout the domain. For the governing differential equation of the form of Eq. (1), boundary conditions that serve this purpose are:

i) Specified primary variable on Γ^p which emanate from a linear potential field as

$$u = a_1 x + a_2 y + a_0$$

or a quadratic field as

$$u = a_1\left(x^2 - y^2\right) + a_2 x + a_3 y + a_0$$

where a_1, a_2, a_3,and a_0 are arbitrary constants.

ii) Specified constant or linear secondary variable on Γ^s

$$q = b_1 x + b_2 y + b_0$$

where b_1, b_2, and b_0 are arbitrary constants.

Consider the solution for the primary variable, $u(x,y)$, in a rectangular domain (see Figure 3(a)) with boundary conditions of the forms indicated that yield the exact solution. The problem is given by Laplace's equation for a planar domain as

$$\frac{\partial^2 u}{\partial x^2} + \frac{\partial^2 u}{\partial y^2} = 0, \qquad 0 < x < a, \qquad 0 < y < b\,.$$

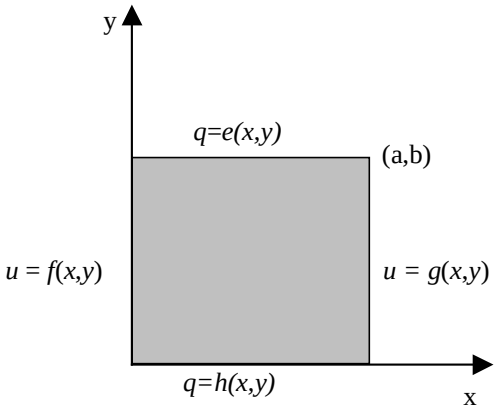

(a) Domain Geometry

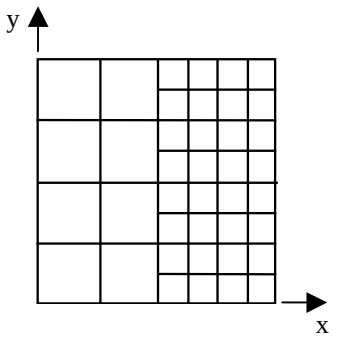

(b) Spatial Discretization

Figure 3. Two-Dimensional Rectangular Domain Geometry and Spatial Discretization.

Specified boundary conditions representing linear, bilinear, and quadratic potential fields are applied to the square domain. These boundary conditions are given as

Linear field:	$u(0,y)=2, \quad u(a,y)=a+2,$ and $q_n(x,0)=q_n(x,b)=0$
Bilinear field:	$u(0,y)=y, \quad u(a,y)=a+y,$ and $q_n(x,0)=-1,$ and $q_n(x,b)=1$
Quadratic field:	$u(0,y)=-y^2, \quad u(a,y)=a^2-y^2,$ $q_n(x,0)=0,$ and $q_n(x,b)=-2b$

Single-domain and multiple-domain spatial modeling approaches are used to analyze the problem. Two single-domain models are developed each using either finite element or finite difference discretization (denoted by SD/FE and SD/FD) over the entire domain. Two multiple-domain models are developed using homogeneous modeling each using either finite element or finite difference discretization (denoted by MD/FE and MD/FD) in each of the subdomains. For convenience, the finite element and finite difference discretizations have the same number of nodes or grid points in each of the coordinate directions in the respective subdomains. A multiple-domain model using heterogeneous modeling (denoted by MD/HM) is developed with finite difference discretization used in one subdomain and finite element discretization used in the other subdomain. For the spatial modeling approaches, the syntax $(m \times n)$ denotes a mesh with m grid points in the x-direction and n grid points in the y-direction. For the single-domain modeling approaches, the entire domain is discretized using a (5×5) grid point mesh.

For the multiple-domain analyses, a (3×5) grid point mesh is used in the less refined (coarse) subdomain and a (5×9) grid point mesh is used in the more refined subdomain as shown in Figure 3(b). Hence, the more refined subdomain has a grid point spacing in the x- and y-directions that is half the size of the spacing used in the coarse subdomain.

Results of the analyses performed have been compared to the exact solution for the given boundary conditions and are summarized in Table 1 using normalized values. A value of unity implies perfect agreement with the reference solution. Values above and below unity indicate error in the computed solution. For boundary conditions consistent with linear and bilinear potential fields, the computed potential and flux results are exact for all analysis types. For boundary conditions consistent with a quadratic potential function, the error in the computed potential and flux is approximately 3% for the multiple-domain homogeneous finite element (MD/FE) spatial modeling, and the error is approximately 1% for the multiple-domain heterogeneous modeling (MD/HM) with combined finite element and finite difference discretization. For the given boundary conditions and element configuration (*i.e.,* square or rectangular elements), the single-domain finite element (SD/FE) model reproduces the exact solution using the bilinear finite element. However, for a general element orientation (*i.e.,* quadrilateral elements), the bilinear element used does not reproduce the exact solution. Moreover, for this problem in the multiple-domain analysis, error is introduced when combining finite element models of different discretization along the common boundary. However, no error is introduced when combining finite different models of different discretization along the common boundary.

Table 1. Results of the Multifunctional Approach for the Patch Test Problems.

Analysis Type*	Normalized Potential Function, u			Normalized Flux, q_x		
	Order of Potential function			Order of Potential Function		
	Linear	Bilinear	Quadratic	Linear	Bilinear	Quadratic
SD/FE	1.0	1.0	1.0	1.0	1.0	1.0
SD/FD	1.0	1.0	1.0	1.0	1.0	1.0
MD/FE	1.0	1.0	1.03	1.0	1.0	1.03
MD/FD	1.0	1.0	1.0	1.0	1.0	1.0
MD/HM	1.0	1.0	.99	1.0	1.0	.99

* SD/FE: Single-Domain with Finite Element discretization
SD/FD: Single-Domain with Finite Difference discretization
MD/FE: Multiple-Domain with Finite Element discretization
MD/FD: Multiple-Domain with Finite Difference discretization
MD/HM: Multiple-Domain with Heterogeneous Modeling (combined finite difference and finite element discretizations)

These results indicate that, for this problem, the finite difference solution better approximates the quadratic potential function. As such, the error obtained using the heterogeneous model (combined finite difference and finite element discretization) is smaller than the error obtained for the homogeneous finite element model.

Representative Benchmark Problem

The multifunctional methodology is demonstrated on a representative two-dimensional scalar-field application. This application is a second-order problem of solid mechanics (*i.e.*, a torsion problem) that can be formulated in terms of one dependent variable (see reference 22 for additional problems).

The torsion of a prismatic bar with a rectangular cross-section is used to demonstrate the multifunctional capabilities of the developed methodology. The torsion problem reduces to the nonhomogeneous partial differential equation

$$\frac{\partial^2 \phi}{\partial x^2} + \frac{\partial^2 \phi}{\partial y^2} = -2G\theta$$

in which the stress function, ϕ, must be constant along the boundary of the cross section, θ is the angle of twist per unit length of the bar, and G is the shear modulus. The configuration of the bar is shown in Figure 4, and the analysis domain and the boundary conditions, are shown in Figure 5(a).

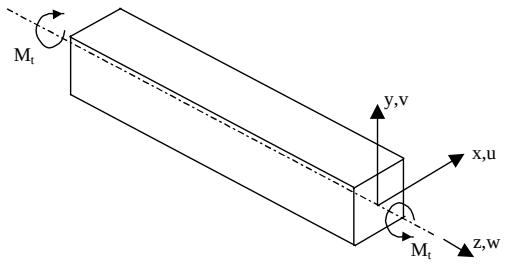

Figure 4. Prismatic Bar with Rectangular Cross-Section.

Due to the symmetries in the problem, only one quadrant of the rectangular cross-section needs to be considered. Moreover, this symmetric model is useful in verifying the application of mixed boundary conditions. That is, the application of boundary conditions in terms of both primary and secondary variables. The quadrant considered in the symmetric model is shown by the gray shaded region in Figure 5(a) and in an enlarged view in Figure 5(b).

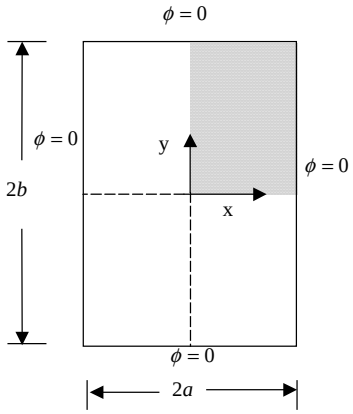

(a) Entire Model

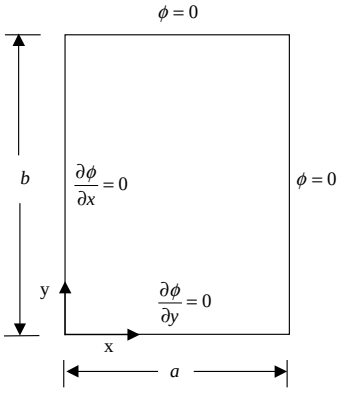

(b) Symmetric Model

Figure 5. Analysis Domains and Boundary Conditions for Prismatic Bar with Rectangular Cross-Section.

The shear stresses in the cross-section are

$$\tau_{zx} = \frac{\partial \phi}{\partial y}, \qquad \tau_{zy} = -\frac{\partial \phi}{\partial x}.$$

At the ends of the bar, the first moment integrated over the cross-sectional area must equal the twisting moment. This requirement gives

$$M_t = 2\int \phi \, dxdy$$

The analytical solution[24] for the stress function and twisting moment are given, respectively, by

$$\phi = \frac{32G\theta a^2}{\pi^3} \sum_{n=1,3,5,\ldots}^{\infty} \frac{1}{n^3}(-1)^{(n-1)/2}\left[1 - \frac{\cosh(n\pi y/2a)}{\cosh(n\pi b/2a)}\right]\cos\frac{n\pi x}{2a}$$

and

$$M_t = \frac{1}{3} G\theta (2a)^3 (2b) \left(1 - \frac{192}{\pi^5} \frac{a}{b} \sum_{n=1,3,5,\ldots}^{\infty} \frac{1}{n^5} \tanh \frac{n\pi b}{2a} \right).$$

Spatial Modeling of Prismatic Bar

Analyses are performed for the case of $b=2a$ (*i.e.*, rectangular cross-section), where a and b are dimensions of the cross-section shown in Figure 5(b). Three levels of grid refinement are used for the spatial modeling, namely meshes of (6×6), (11×11), and (21×21) grid points, each applied to the domain shown in Figure 5(b). A typical idealization for a (6×6) mesh of grid points is shown in Figure 6(a). Multiple-domain analyses with the spatial modeling of these three levels of grid refinement and with coincident nodes along the common subdomain boundary have been performed for comparison. For the multiple-domain spatial modeling with non-coincident nodes along the common boundary, the mesh discretization of the most refined domain is consistent with the discretization used in that same region for the single-domain analysis. The mesh in the less refined domain has half the "element" density of that used in the refined domain. The mesh of the entire domain is shown in Figure 6(b) and is referred to by the syntax (6×11)/(11×21).

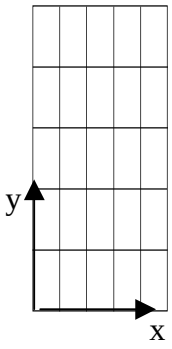

(a) Single-Domain (6×6) Mesh

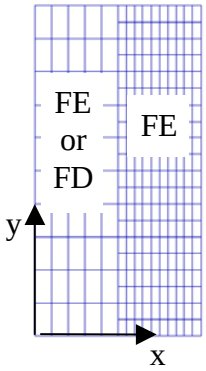

(b) Multiple-Domain (6×11)/(11×21) Mesh

Figure 6. Spatial Discretization for One Quadrant of Prismatic Bar with Rectangular Cross-Section

Twisting Moment for the Prismatic Bar

Having found the values of the stress function, ϕ, at the grid points in the solution domain by the respective spatial discretization approaches, the twisting moment may be found by repeated application of the trapezoidal rule for numerical integration. The computed twisting moment, M_t, is normalized by the analytical solution, $M_{t\,analytical}$, and is given in Table 2. A value of unity indicates perfect agreement with the analytical solution. Values above and below unity indicate error in the computed solution. Results in Table 2 indicate that all analyses are in good agreement with the analytical solution. The maximum error in any of the computed solutions is approximately 5% and is observed for the multiple-domain heterogeneous modeling analysis (MD/HM) using combined finite difference and finite element discretizations with the (6×6) mesh of grid points with coincident nodes along the common boundary. The maximum error in this analysis is due to a combination of the discretization error and error in the multifunctional approach for combining the finite element and finite difference meshes.

The error for the multiple-domain analyses using combined finite difference and finite element discretizations (MD/HM) with noncoincident grid points along the common boundary is less than 3%. The solution accuracy for each of the modeling methods increases as the mesh refinement increases. For the same number of nodes or grid points, the finite element discretization yields more accurate solutions than the finite difference discretization.

The results obtained for the single-domain modeling (*e.g.*, SD/FE and SD/FD) and the multiple-domain homogeneous modeling with coincident nodes along the subdomain boundary are identical or nearly identical (see the results for (6×6), (11×11) and (21×21) meshes in Table 2). The results obtained for the multiple-domain heterogeneous modeling approach (MD/HM) with coincident grid points along the subdomain boundary are less accurate than corresponding results obtained using homogeneous modeling (MD/FE and MD/FD) but are in overall good agreement. With multiple-domain modeling using finite element (MD/FE) discretization and with non-coincident nodes, the twisting moment obtained is bounded by the twisting moments obtained using the less refined (11×11) and more refined (21×21) coincident meshes (see the results for the (6×11)/(11×21) mesh in Table 2). For the multiple-domain finite difference (MD/FD) discretization in both domains

Table 2. Normalized Twisting Moment for Prismatic Bar.

Analysis Type*	Normalized Twisting Moment, $M_t/(M_t)_{analytical}$			
	Mesh Density			
	(6×6)	(11×11)	(21×21)	$(6 \times 11)/(11 \times 21)$
SD/FE	0.987	0.994	0.998	-
SD/FD	0.974	0.990	0.996	-
MD/FE	0.987	0.994	0.998	0.996
MD/FD	0.975	0.990	0.996	0.983
MD/HM	0.950	0.974	0.988	0.975

* SD/FE: Single-Domain with Finite Element discretization
SD/FD: Single-Domain with Finite Difference discretization
MD/FE: Multiple-Domain with Finite Element discretization
MD/FD: Multiple-Domain with Finite Difference discretization
MD/HM: Multiple-Domain with Heterogeneous Modeling (combined finite difference and finite element discretizations)

with non-coincident nodes, the twisting moment is slightly less accurate than the results obtained using the (11×11) coincident mesh, which is indicative of the error introduced by the finite difference interface constraints along the common boundary. For the heterogeneous modeling approach with coincident nodes along the interface boundary, the twisting moment is less accurate than the homogeneous approach with either finite element modeling or finite difference modeling. These results reveal the error introduced in the heterogeneous modeling approach for this problem due to the interface constraints. For the heterogeneous modeling approach with non-coincident nodes, the twisting moment is slightly more accurate than the (11×11) coincident mesh, which is indicative of the benefit gained (*i.e.*, more accurate field approximation and interface constraint) by the combination of the finite element and finite difference discretizations.

Concluding Remarks

Multifunctional methodologies have been formulated for interfacing diverse domain idealizations including multi-fidelity modeling and multiple spatial modeling approaches. The methods, based on the method of weighted residuals, provide accurate compatibility of primary and secondary variables across domain interfaces as shown for several problems. The methodology has been described and demonstrated for the illustrative problems. These selected problems include a verification test case and a second-order problem of solid mechanics that can be formulated in terms of one dependent variable. The governing equation in each case is either the Laplace or the Poisson equation. In all cases considered, the results obtained using the multifunctional methodology were in overall good agreement with the reported analytical or reference solution. The methods have been rigorously developed for multiple-domain applications, and the robustness and accuracy has been illustrated, and the associated computational issues have been discussed. Multi-fidelity modeling approaches have been developed that include both homogeneous (*i.e.*, the same discretization method in each domain) and heterogeneous (*i.e.*, different discretization methods in each domain) discretization approaches. The finite element and finite difference methods and combinations thereof have been used in each of the discretization approaches. Results have been presented for the two-dimensional scalar-field multifunctional formulation using representative test problems in solid mechanics.

References

1. Ransom, J. B., *Global/Local Stress Analysis of Composite Structures*, M.S. Thesis, Department of Mechanical Engineering and Mechanics, Old Dominion University, 1989. (Available as NASA TM-101640.)

2. Ransom, J. B. and Knight, N. F., Jr., "Global/Local Stress Analysis of Composite Panels," *Computers and Structures*, Vol. 37, No. 4, 1990, pp. 375-395.

3. Whitcomb, J. D. and Kyeongsik, W., "Application of Iterative Global/Local Finite Element Analysis, Part 1: Linear Analysis," *Communications in Numerical Methods in Engineering*, Vol. 9, 1993, pp. 745-756.

4. Whitcomb, J. D. and Kyeongsik, W., "Application of Iterative Global/Local Finite Element Analysis, Part 2: Geometrically Nonlinear Analysis,"

Communications in Numerical Methods in Engineering, Vol. 9, 1993, pp. 757-766.

5. Farhat, C. and Riux, F.-X., "A Method of Finite Element Tearing and Interconnecting and Its Parallel Solution Algorithm," *International Journal for Numerical Methods in Engineering*, Vol. 32, No. 6, 1991, pp. 1205-1228.

6. Quiroz, L. and Beckers, P., "Non-conforming Mesh Gluing in the Finite Element Method," *International Journal for Numerical Methods in Engineering*, Vol. 17, 1995, pp. 186-195.

7. Pantano, A. and Averill, R. C., "A Finite Element Interface Technology for Modelling Delamination Growth in Composite Structures," AIAA Paper No. 2002-1662, *Proceedings of the AIAA/ASME/ASCE/AHS/ASC 43rd Structures, Structural Dynamics, and Materials Conference*, 2002, pp. 1862-1872.

8. Dohrmann, C. R., Key, S. W., and Heinstein, M. W., "A Method of Connecting Dissimilar Finite Element Meshes in Two Directions," *International Journal for Numerical Methods in Engineering*, Vol. 48, 2000, pp. 655-678.

9. Housner, J. M. and Aminpour, M. A., "Multiple Methods Integration for Structural Mechanics Analysis and Design," *First NASA Advanced Composites Technology Conference*, NASA CP 3104, Part 2, 1991, pp. 875-889.

10. Aminpour, M. A., Ransom, J. B., and McCleary, S. L., "A Coupled Analysis for Structures with Independently Modeled Finite Element Subdomains," *International Journal for Numerical Methods in Engineering*, Vol. 38, 1995, pp. 3695-3718.

11. Krishnamurthy, T. and Raju, I. S., "Coupling Finite and Boundary Element Methods for Two-Dimensional Potential Problems," AIAA Paper No. 92-2240, *Proceedings of the AIAA/ASME/ASCE/AHS/ASC 33rd Structures, Structural Dynamics, and Materials Conference*, 1992, pp. 148-162.

12. Krishnamurthy, T. and Raju, I. S., "Coupling Finite and Boundary Element Methods for 2-D Elasticity Problems," AIAA Paper No. 93-1451, *Proceedings of the AIAA/ASME/ASCE/AHS/ASC 34th Structures, Structural Dynamics, and Materials Conference*, 1993, pp. 1274-1290.

13. Pates, C. S., Mei, C., and Shirahatti, U., "Coupled Boundary/Finite Element Methods for Random Structural-Acoustic Vibrations," AIAA Paper No. 95-1346, *Proceedings of the AIAA/ASME/ASCE/AHS/ASC 36th Structures, Structural Dynamics, and Materials Conference*, 1995, pp. 1569-1579.

14. Zienkiewicz, O. C., Kelly, D. W., and Peters, P., "The Coupling of the Finite Element Method and Boundary Solution Procedures," *International Journal for Numerical Methods in Engineering*, Vol. 11, 1977, pp. 355-375.

15. Kao, P., "Coupled Rayleigh-Ritz/Finite Element Structural Analysis Using Penalty Function Method," AIAA Paper No. 92-2238, *Proceedings of the AIAA/ASME/ASCE/AHS/ASC 33rd Structures, Structural Dynamics, and Materials Conference*, 1992, pp. 135-139.

16. Holt, M. and Meade, A. J., Jr., "Flight Vehicle Aerodynamics Calculated by a Galerkin Finite Element/Finite Difference Method," *Computing Systems in Engineering*, Vol. 3, Nos. 1-4, 1992, pp. 413-421.

17. Dow, J. O., Hardaway, J. L., and Hamernik, J. D., "Combined Application of the Finite Element/Finite Difference Methods," AIAA Paper No. 92-2237, *Proceedings of the AIAA/ASME/ASCE/AHS/ASC 33rd Structures, Structural Dynamics, and Materials Conference*, 1992, pp. 129-134.

18. Rao, A. K., Raju, I. S., and Murty, A. V. K., "A Powerful Hybrid Method in Finite Element Analysis," *International Journal for Numerical Methods in Engineering*, Vol. 3, 1971, pp. 389-403.

19. Giles, G. L. and Norwood, R. K., "Coupling Equivalent Plate and Finite Element Formulations in Multiple-Method Structural Analyses," *AIAA Journal of Aircraft*, Vol. 31, No. 5, 1994, pp. 1189-1196.

20. Ransom, J. B., McCleary, S. L., and Aminpour, M. A., "A New Interface Element for Connecting Independently Modeled Substructures," AIAA Paper No. 93-1503, *Proceedings of the*

AIAA/ASME/ASCE/AHS/ASC 34th Structures, Structural Dynamics, and Materials Conference, 1993, pp. 1693-1703.

21. Reddy, J. N., *An Introduction to the Finite Element Method*, McGraw-Hill Book Company, New York, 1984.

22. Ransom, J. B., *On Multifunctional Collaborative Methods in Engineering Science*, Ph.D. Dissertation, Department of Aerospace Engineering, Old Dominion University, 2001. (Available as NASA TM-2001-211046.)

23. Moas, E. (Editor), *The COMET-AR Users Manual*, NASA CR-97-206248, 1997.

24. Timoshenko, S. P. and Goodier, J. N., *Theory of Elasticity*, Third Edition, McGraw-Hill, New York, 1970.